



Synthesis and photoluminescence analysis of $Y_{1.50}Sc_{0.50}O_3:Sm^{3+}$ and $Y_{1.50}Sc_{0.50}O_3:Dy^{3+}$ phosphors

Esra Öztürk* & Erkul Karacaoglu

Karamanoğlu Mehmetbey University, Engineering Faculty, Department of Metallurgical and Materials Engineering, Karaman, Turkey

*E-mail: esracircir@gmail.com

Received 29 January 2021; revised and accepted 01 May 2021

In this study, $Y_{1.50}Sc_{0.50}O_3:Sm^{3+}$ and $Y_{1.50}Sc_{0.50}O_3:Dy^{3+}$ have been synthesized by a solid state reaction method and their photoluminescence (PL) properties have been investigated. Single-phase and well-crystallized cubic $Y_{1.50}Sc_{0.50}O_3:Sm^{3+}$ and $Y_{1.50}Sc_{0.50}O_3:Dy^{3+}$ phosphors are obtained after calcinations at 800 °C and 900 °C for 6 h. X-ray diffraction patterns confirm that both phosphors have a cubic phase without secondary phase. According to scanning electron microscope results, the particle size of both phosphors exhibit relatively irregular and their particle size are determined to be between 0.27 μm –0.70 μm and 0.25 μm –2.04 μm for $Y_{1.50}Sc_{0.50}O_3:Sm^{3+}$ and $Y_{1.50}Sc_{0.50}O_3:Dy^{3+}$, respectively. The PL excitation and emission spectra are recorded for both types of the phosphors. Emission spectra of $Y_{1.50}Sc_{0.50}O_3:Sm^{3+}$ and $Y_{1.50}Sc_{0.50}O_3:Dy^{3+}$ are found to be typical for Sm^{3+} and Dy^{3+} .

Keywords: Y_2O_3 , Solid solutions, Photoluminescence, Dopants/doping

The rare earth (RE) ion doped phosphors are considered as advanced materials which serve unique spectroscopic properties, namely narrow emission bandwidths, large Stokes shifts, suitability for multi-photon excitation and long fluorescence lifetimes. They have been used in different applications, such as photoluminescent and opto-electronic devices, catalysts, sensors, fluorescent labels, etc. due to their optical characteristics based on the 4f–5d electron transition¹. Until today, yttrium oxide (Y_2O_3) is found to be one of the optimal promising host crystal for doping RE ions, because of its chemical property and ionic radius similarities. This structure has high melting point (~2600 °C), wide transparency range, high chemical stability with a band gap (5.72 eV) and down- and up-conversion luminescence with high efficiency²⁻⁴. On the other hand, trivalent RE ions have been extensively studied in various hosts due to their unique luminescent properties. Recently, considerable studies have been carried out to examine RE ions-doped Y_2O_3 materials since they exhibit remarkably different luminescence properties. Particularly, Eu^{3+} -activated Y_2O_3 phosphor is a well-known red emitting phosphor that is suitable to use in field emission displays, fluorescent lights and cathode-ray tubes⁵⁻⁶.

In this research, Sc^{3+} substituted and Sm^{3+} and Dy^{3+} -doped $Y_{1.50}Sc_{0.50}O_3$ phosphors were synthesized

successfully by solid state reaction method (ceramic method) in open atmosphere. Sc^{3+} ion present an ionic radius about 0.75 Å compared to Sm^{3+} and Dy^{3+} having ionic radius= 1.07 Å and 1.03 Å, respectively. Generally, this property results as enhancing crystal field strength for those dopants, silicates, and oxides⁷.

Material and Methods

The samples which have general formula $(Y_{1-x}RE_x)_{1.50}Sc_{0.50}O_3$ with following composition $(1.5-x)Y_{1.50}Sc_{0.50}O_3 + xSm_2O_3$ and $(1.5-x)Y_{1.50}Sc_{0.50}O_3 + xDy_2O_3$, where $x= 0.05$ and were produced by a solid state reaction method. The starting materials of high purity Y_2O_3 (99.9%, Acros Organics), Scandium(III) oxide (Sc_2O_3 , 99.9%, abcr chemicals), Samarium(III) oxide (Sm_2O_3 , 99.9%, Aldrich) and Dysprosium(III) oxide (Dy_2O_3 , ≥99.99%, Aldrich) were chosen to synthesize phosphors. The starting materials were stoichiometrically calculated and grinded in an agate mortar. The thermal properties of the compositions were analyzed at a heating rate of 10 °C/min from 50 °C to 1400 °C by differential thermal analysis (DTA) and thermogravimetric (TG) instrument (SII Nanotechnology SII 6000 Exstar TG/DTA 6300). Pure alumina crucibles were used for the heat treatments which were performed in a muffle furnace (Protherm PLF120/5) under open atmosphere. The sintered samples were grinded to powder form

for the characterizations. The phase formation examinations were done with Bruker AXS D8 Advance model X-ray diffractometer (XRD), which run at 40 kV and 30 mA (Cu-K α radiation) in a step-scan mode ($0.02^\circ/2\theta$). The morphology of particles and elemental analysis (EDX) of samples were investigated by a scanning electron microscope (SEM). Eventually, the photoluminescence (PL) studies including the excitation and emission spectra and fluorescence decay curves as well as lifetimes were analysed by a spectrofluorometer (Photon Technology International, QuantaMasterTM 30).

Results and Discussion

Thermal analysis

The thermal behaviours of $Y_{1.40}Sm_{0.10}Sc_{0.50}O_3$ and $Y_{1.40}Dy_{0.10}Sc_{0.50}O_3$ phosphors were determined in the range 50 to 1400 °C and the plots are given in Fig. 1. DTA/TG curves of $Y_{1.40}Sm_{0.10}Sc_{0.50}O_3$ in Fig. 1a consist of DTA/TG curves of pure Sm_2O_3 ⁸ and a mass loss of 1.2 weight% observed between 50–475 °C was associated with the removal of water adsorbed by the material due to the foam-like morphology $Sm(III)$ oxide. However, the Dy^{3+} -doped $Y_{1.40}Sc_{0.50}O_3$ composition does not show any mass loss or endo/exo-thermic reaction up to 1400 °C (Fig. 1b).

X-ray diffraction (XRD) analysis

Firstly, a pre-heat treatment process was applied at 800 °C for 6 h, then the heat treatment at 1000 °C for 6 h was applied for single phase formation. After the sintering process, the XRD analyses were conducted for both samples. The Fig. 2 shows the comparative XRD patterns of $Y_{1.40}Sm_{0.10}Sc_{0.50}O_3$ and $Y_{1.40}Dy_{0.10}Sc_{0.50}O_3$ phosphors. The phosphor samples were clearly indexed by cubic phase of Y_2O_3 (JPCDS cards No.- 00-043-1036). In this case no evidence of

the secondary phase was observed, the heat treatments were enough to get single phase of host crystal. Additionally, the diffraction peaks become sharper as the temperature is enough, as an effect of crystallinity enhancement and there was no evidence change in peak positions in spite of the doping of Sm^{3+} and Dy^{3+} ions. Furthermore, Y_2O_3 is indexed for all samples although the composition was $Y_{1.50}Sc_{0.50}O_3$, initially. Moreover, small amounts of Sm^{3+} and Dy^{3+} dopant ions have been incorporated into the host lattice and caused any distortions in the lattice structure or any secondary phase formations as it can be clearly seen in unaltered and similar diffraction patterns. The phosphors were well-crystallized in the cubic structure and the lattice parameters are $a = b = c = 9.845 \text{ \AA}$, $\alpha = 90^\circ$, $\beta = 90^\circ$ and $\gamma = 90^\circ$.

SEM-EDX analysis

SEM images and EDX results of synthesized $Y_{1.40}Sm_{0.10}Sc_{0.50}O_3$ and $Y_{1.40}Dy_{0.10}Sc_{0.50}O_3$ phosphors are shown in Fig. 3. The particle size distribution measured directly from SEM images were approximately in the

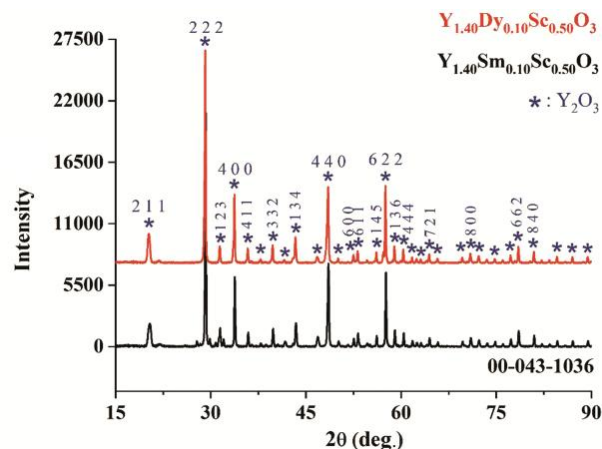


Fig. 2 — The comparative XRD patterns of $Y_{1.40}Sm_{0.10}Sc_{0.50}O_3$ and $Y_{1.40}Dy_{0.10}Sc_{0.50}O_3$

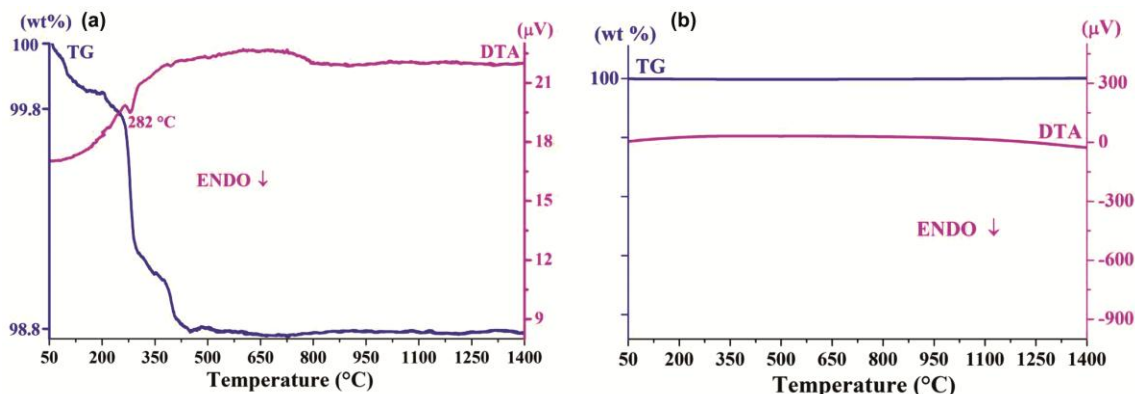


Fig. 1 — DTA/TG plots of (a) $Y_{1.40}Sm_{0.10}Sc_{0.50}O_3$ and $Y_{1.40}Dy_{0.10}Sc_{0.50}O_3$

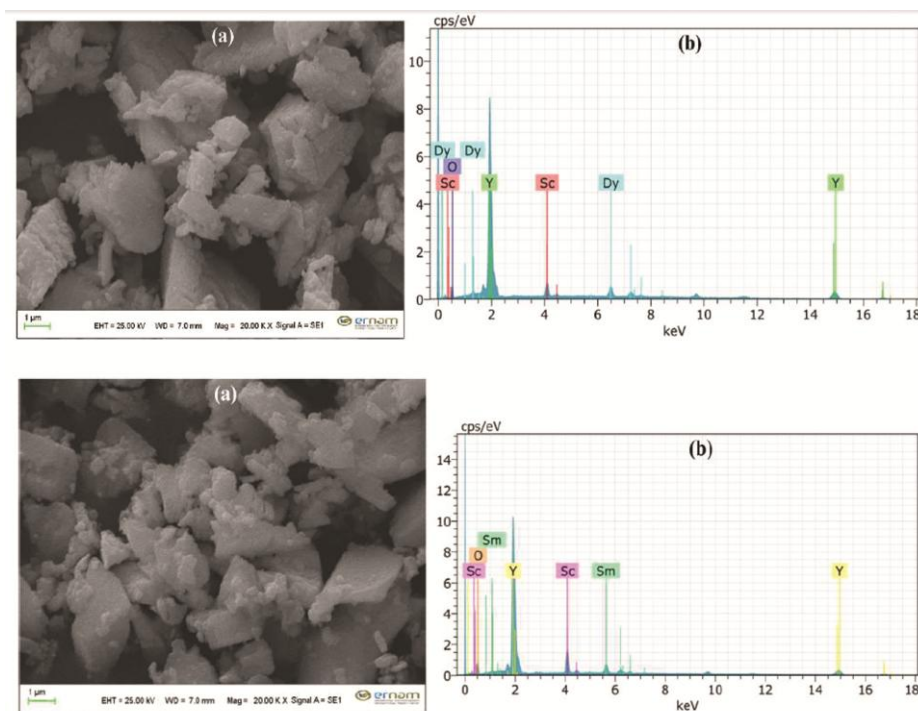


Fig. 3 — SEM images (a and b) and EDX plots (c and d) of $Y_{1.40}Sm_{0.10}Sc_{0.50}O_3$ (upper panel) and $Y_{1.40}Dy_{0.10}Sc_{0.50}O_3$ (lower panel) phosphor

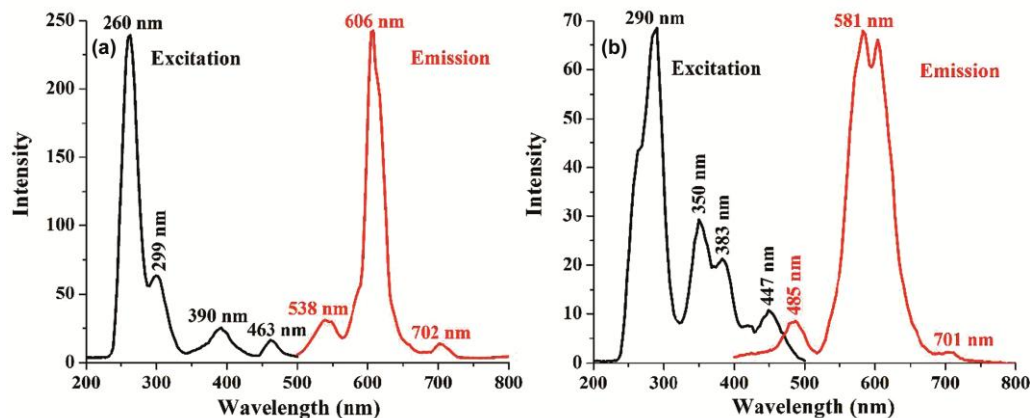


Fig. 4 — PL spectra of (a) $Y_{1.40}Sm_{0.10}Sc_{0.50}O_3$ and (b) $Y_{1.40}Dy_{0.10}Sc_{0.50}O_3$ phosphors

ranges of 0.27 – 0.70 μm and 0.25 – 2.04 μm for $Y_{1.40}Sm_{0.10}Sc_{0.50}O_3$ and $Y_{1.40}Dy_{0.10}Sc_{0.50}O_3$ phosphors, respectively. The micron size particles of both samples have relatively irregular and agglomerated morphology, and composed of individual small particles with a rounded morphology. According to EDX results, the Sm and Dy element peaks had low intensities because their low quantities in compositions as expected.

Photoluminescence properties

The PL spectra of samples are given in Fig. 4. The excitation spectra of samples were recorded in the

range of 200-500 nm using $\lambda_{\text{emission}} = 606 \text{ nm}$ for Sm^{3+} -doped and $\lambda_{\text{emission}} = 581 \text{ nm}$ for Dy^{3+} -doped phosphor. Sm^{3+} has $4f^5$ configuration and complicated energy levels and diverse possible transitions between f-levels, so the transitions between f-levels are highly selective and have sharp line spectra. The excitation spectrum of $Y_{1.40}Sm_{0.10}Sc_{0.50}O_3$ which is shown in Fig. 4a has more than one peaks. The maximum excitation band in the range 260-290 nm are related with $Sm^{3+}-O^{2-}$ charge transfer transitions⁹. The peaks at 390 nm and 463 nm are due to the excitation from ground-level ${}^6H_{5/2}$ to higher energy levels (${}^6P_{7/2}$ and

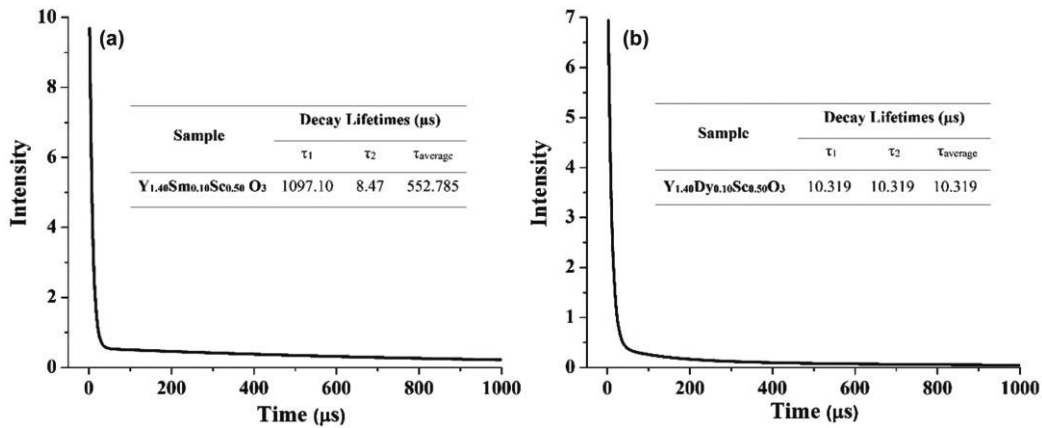


Fig. 5 — Luminescence decay curves (a) by monitoring the ${}^4G_{5/2} \rightarrow {}^6H_{7/2}$ transition at ~ 606 nm in $Y_{1.40}Sm_{0.10}Sc_{0.50}O_3$ and (b) by monitoring the ${}^4F_{9/2} \rightarrow {}^6H_{13/2}$ transition at ~ 581 nm in $Y_{1.40}Dy_{0.10}Sc_{0.50}O_3$ phosphor

${}^4F_{5/2} + {}^4I_{13/2}$) of Sm^{3+} ion⁹⁻¹¹. The PL emission spectrum of Sm^{3+} -doped phosphor in red region consists of three peaks near 538 nm, 606 nm and 702 nm, which are assigned to the intra-4f-shell transitions from the excited level ${}^4G_{5/2}$ to ground levels ${}^6H_{5/2}$ ⁽⁹⁻¹²⁾, ${}^6H_{7/2}$ ⁽⁹⁻¹²⁾, ${}^6H_{11/2}$ ⁽¹¹⁻¹²⁾, respectively.

It is proved with various phosphors (hosts) in previous studies that the emission colour of the trivalent dysprosium, Dy^{3+} ($4f_9$ configuration) photoluminescence is close to white. The excitation and emission spectra of $Y_{1.40}Dy_{0.10}Sc_{0.50}O_3$ phosphor which are shown in Fig. 4b, has the strongest excitation at 290 nm and assigned to ${}^6H_{15/2} \rightarrow {}^4K_{13/2} + {}^4H_{13/2}$ transitions of Dy^{3+} . The peak at 350 nm is attributed to the hypersensitive transition ${}^6H_{15/2} \rightarrow {}^4M_{15/2} + {}^6P_{7/2}$ and other bands with peaks at 383 nm and 447 nm are related with ${}^6H_{15/2} \rightarrow {}^4I_{13/2}$ and ${}^6H_{15/2} \rightarrow {}^4I_{15/2}$ transitions, respectively. The yellowish white light emission of this phosphor is composed of blue (485 nm) and yellow (581 nm) colour regions and recorded under excitation of 290 nm. These emissions correspond to the transitions from the ${}^4F_{9/2}$ excited state to the ${}^6H_{15/2}$ and ${}^6H_{13/2}$ (corresponds to the hypersensitive transition) ground states, respectively^{4, 9, 14-15}.

Luminescence decay curves of samples recorded at $\lambda_{em} = 606$ nm and $\lambda_{em} = 581$ nm are shown in Fig. 5. All the data for every sample are wellfitted with the following double exponential decay:

where, I_0 and I are the luminescence intensity at initial time and at time t , respectively, A_1 and A_2 are constants, τ_1 and τ_2 are the decay time for the

exponential components, respectively. Results for fitted decay curve of samples are given in the inset of the respective figures. The $\tau_{average}$ results show that Sm^{3+} -doped phosphor has longer lifetime of 552.785 μs than Dy^{3+} -doped one with $\tau_{average} = 10.319$ μs .

Conclusions

The $Y_{1.40}Sm_{0.10}Sc_{0.50}O_3$ and $Y_{1.40}Dy_{0.10}Sc_{0.50}O_3$ phosphors were synthesized by solid-state reaction method under open atmosphere resulting single phase ($Y_{1.50}Sc_{0.50}O_3$) and completely indexed with Y_2O_3 host lattice. It can be said that the Sc^{3+} -ions are substituted in Y_2O_3 host lattice. XRD studies showed that $Y_{1.40}Sm_{0.10}Sc_{0.50}O_3$ and $Y_{1.40}Dy_{0.10}Sc_{0.50}O_3$ phosphors have cubic crystal structure with high crystallinity. The particle size distributions were measured as 0.27 μm –0.70 μm and 0.25 μm –2.04 μm for $Y_{1.40}Sm_{0.10}Sc_{0.50}O_3$ and $Y_{1.40}Dy_{0.10}Sc_{0.50}O_3$ phosphors, respectively. The excitation spectra of both phosphors are in the UV-region below 300 nm and this phenomenon also confirms that the Sm^{3+} and Dy^{3+} interactions with host lattice are very strong. Thus, we can say that the energy transfer occurs between Sm^{3+}/Dy^{3+} ions and the host crystal ($Y_{1.50}Sc_{0.50}O_3$). The emission bands of phosphors are also well compatible with the related dopant ions in phosphors. So, synthesized phosphors in this study could be considered as candidate for white-emitting devices.

Acknowledgement

The authors would like to thank Karamanoglu Mehmetbey University, Scientific Research Projects Commission (BAP, project number: 11-M-17), Republic of Turkey, for financial support. The authors are grateful to Prof. Dr. Adil Denizli from

Hacettepe University, Department of Chemistry and Biochromatography and Biodiagnostics Research Group for their kind help.

References

- 1 Öztürk E & Karacaoglu E, *J Therm Anal Calorim*, 131(2018) 2261.
- 2 Velazquez D Y M, Soto L A H, Ramirez Á de J M, Carmona-Téllez S, Garfias-Garcia E, Falcony C & Murillo A G, *Ceram Int*, 41 (2015) 8481.
- 3 Li X, Chen Y, Qian Q, Liu X, Xiao L & Chen Q, *J Lumin*, 132 (2012) 81.
- 4 Shivaramu N J, Nagabhushana K R, Lakshminarasappa B N & Singh F, *J Lumin*, 169 (2016) 627.
- 5 Uzun E, Öztürk E, Kalaycioglu Ozpozan N & Karacaoglu E, *J Lumin*, 173 (2016) 73.
- 6 Muresana L, Popovici E J, Imre-Lucacia F, Grecu R & Indrea E, *J Alloy Compd*, 483 (2009) 346.
- 7 Najjar A, Omi H & Tawara T, *Nanoscale Res Lett*, 9(2014) Article 356.
- 8 Ruiz-Gómez M A, Gómez-Solís C, Zarazúa-Morín M E, Torres-Martínez L M, Juárez-Ramírez I, Sánchez-Martínez D & Figueroa-Torres M Z, *Ceram Int*, 40 (2014) 1893.
- 9 Li Y-C, Chang Y-H, Lin Y-F, Chang Y-S & Lin Y-J, *J Alloy Compd*, 439 (2007) 367.
- 10 Zhang F, Wang Y & Tao Y, *Mater Res Bull*, 48 (2013) 1952.
- 11 Naresh V & Buddhudu S, *J Lumin*, 147 (2014) 63.
- 12 Deng H, Zhao Z, Wang J, Hei Z, Li M, Noh H M, Jeong J H & Yu R, *J Solid State Chem*, 228 (2015) 110.
- 13 Krishn K M, Anoop G & Jayaraj M K, *J Electrochem Soc*, 154 (2007) J310.
- 14 Babu P, Jang K H, Kim E S, Shi L & Seo H J, *J Korean Phys Soc*, 54 (2009) 1488.
- 15 Shen W Y, Pang M L, Lin J & Fang J, *J Electrochem Soc*, 152 (2005) H25.